

Vector Theory of Cross-Phase Modulation: Role of Nonlinear Polarization Rotation

Qiang Lin and Govind P. Agrawal, *Fellow, IEEE*

Abstract—We develop a vector theory of cross-phase modulation (XPM) capable of describing nonlinear coupling between two pulses of different wavelengths and arbitrary states of polarization. We focus for simplicity on the pump-probe configuration and use it to investigate the temporal and spectral polarization effects occurring inside an optical fiber. Using the Stokes-vector formalism we show that the probe polarization changes in general through XPM-induced nonlinear polarization rotation. In the absence of dispersion-induced probe broadening, such nonlinear changes in the probe polarization do not affect the temporal shape of the probe pulse but produce a multipeak spectrum whose different spectral peaks have different states of polarization. When dispersive effects are included, even the shape of the probe pulse becomes polarization dependent, and different parts of the pulse develop different states of polarization. Such nonlinear polarization effects lead to novel phenomena such as polarization-dependent compression and splitting of the probe pulse.

Index Terms—Cross-phase modulation (XPM), nonlinear optics, optical fiber polarization, polarization.

I. INTRODUCTION

CROSS-PHASE modulation (XPM) is a nonlinear phenomenon occurring when two or more optical waves are transmitted simultaneously through a nonlinear medium such as an optical fiber [1]. Physically, each intense optical wave changes the refractive index of fiber through the Kerr effect and induces a nonlinear phase shift on other copropagating waves. If this wave is in the form of an optical pulse, the XPM-induced nonlinear phase shift becomes time dependent and leads to spectral broadening of the copropagating waves. The XPM phenomenon in optical fibers has been studied extensively over the last two decades [2]–[12] and is widely used as a mechanism for optical switching and wavelength conversion [13]–[19]. However, much less attention has been paid to the polarization effects occurring when two optical pulses at different carrier frequencies interact with each other through XPM inside an isotropic fiber, even though the polarization-dependent nature of XPM is well known [20].

The theoretical development of XPM has so far considered the nonlinear coupling either between two polarization components of a single optical field or between the identically polarized components of two optical fields at different frequencies [1]. In the latter case, it is assumed that the two fields remain

copolarized throughout the fiber so that a scalar theory of XPM can be used. This assumption is questionable even for an ideal isotropic fiber (no birefringence) when the fields are elliptically polarized initially because of a phenomenon known as nonlinear polarization rotation (NPR), which can change the state of polarization (SOP) of an optical field through XPM. In the case of two noncopolarized optical pulses, XPM not only induces different nonlinear phase shifts for the two polarization components but also transfers energy between them although the total power remains conserved. As a result, the SOP of each wave becomes nonuniform, both temporally and spectrally in a way that is much different from the scalar case. It is important to investigate the XPM effect on optical pulses with arbitrary polarizations because it is hard to maintain copolarization between two pulses inside a fiber unless a high-birefringence fiber is used.

In this paper, we develop a vector theory of XPM and use it to investigate the temporal and spectral polarization effects occurring when two optical pulses with different wavelengths and different states of polarization are launched into an optical fiber. The paper is organized as follows. We use the Jones-matrix formalism in Section II to derive a set of two vector (or four scalar) coupled nonlinear Schrödinger (NLS) equations. In Section III we focus for simplicity on the pump-probe configuration, neglect pulse broadening induced by group-velocity dispersion (GVD), but include the group-velocity mismatch between the pump and probe pulses owing to their different wavelengths. Using the Stokes-vector formalism, we study in this section how the SOPs of the pump and probe change on the Poincaré sphere. Section IV focuses on the XPM-induced spectral broadening and shows that different spectral peaks of the probe pulse in general do not have the same SOP. The GVD effects are allowed in Section V where we focus on the temporal shape of the probe pulse and discuss intrapulse polarization effects. The main results are summarized in Section VI.

II. VECTOR THEORY OF XPM

In this section we use the Jones-matrix formalism to derive a set of two vector NLS equations that are not only coupled nonlinearly through XPM but also include the effects of self-phase modulation (SPM) and GVD. The SPM and XPM phenomena have their origin in the third-order nonlinear effects [20]. Assuming an instantaneous electronic response and neglecting the Raman contribution, the third-order nonlinear polarization in a medium such as silica glass is given by [1]

$$P^{(3)}(\mathbf{r}, t) = \epsilon_0 \chi^{(3)} : \mathbf{E}(\mathbf{r}, t) \mathbf{E}(\mathbf{r}, t) \mathbf{E}(\mathbf{r}, t) \quad (1)$$

Manuscript received November 4, 2003; revised March 10, 2004. This work is supported in part by the National Science Foundation under Grant ECS-0320816 and Grant DMS-0073923.

The authors are with the Institute of Optics, University of Rochester, Rochester, NY 14627 USA (e-mail: linq@optics.rochester.edu).

Digital Object Identifier 10.1109/JQE.2004.830198

where ϵ_0 is the vacuum permittivity, \mathbf{E} is the electric field vector, and the tensor $\overset{\leftrightarrow}{\chi}^{(3)}$ represents the third-order susceptibility of the nonlinear medium.

In the case of two distinct optical fields propagating simultaneously inside an optical fiber, the total electric field can be written as

$$\mathbf{E} = \text{Re}[\mathbf{E}_1 \exp(-i\omega_1 t) + \mathbf{E}_2 \exp(-i\omega_2 t)] \quad (2)$$

where Re stands for the real part and \mathbf{E}_j is the slowly varying (complex) amplitude for the field oscillating at frequency ω_j ($j = 1, 2$). Writing $\mathbf{P}^{(3)}$ also in the same form as

$$\mathbf{P}^{(3)} = \text{Re}[\mathbf{P}_1 \exp(-i\omega_1 t) + \mathbf{P}_2 \exp(-i\omega_2 t)] \quad (3)$$

and assuming an isotropic nonlinear medium, the nonlinear polarization \mathbf{P}_j at frequency ω_j is found to be

$$\begin{aligned} \mathbf{P}_j = & \frac{\epsilon_0}{4} \chi_{1111}^{(3)} [(\mathbf{E}_j \cdot \mathbf{E}_j) \mathbf{E}_j^* + 2(\mathbf{E}_j^* \cdot \mathbf{E}_j) \mathbf{E}_j \\ & + 2(\mathbf{E}_m^* \cdot \mathbf{E}_m) \mathbf{E}_j + 2(\mathbf{E}_m \cdot \mathbf{E}_j) \mathbf{E}_m^* \\ & + 2(\mathbf{E}_m^* \cdot \mathbf{E}_j) \mathbf{E}_m] \end{aligned} \quad (4)$$

where $j, m = 1$ or 2 ($j \neq m$), and we used the fact that the tensor $\overset{\leftrightarrow}{\chi}^{(3)}$ has only four nonzero components for an isotropic medium and that they are related to each other as $\chi_{1122}^{(3)} = \chi_{1212}^{(3)} = \chi_{1221}^{(3)} = \chi_{1111}^{(3)}/3$.

The two optical fields \mathbf{E}_1 and \mathbf{E}_2 evolve along the fiber length as dictated by the combination of GVD, SPM, and XPM. It is common to choose the z axis along the fiber axis and assume that \mathbf{E}_1 and \mathbf{E}_2 lie in the x - y plane. This assumption amounts to neglecting the longitudinal component of the field vectors and is justified in practice as long as the spatial size of the fiber mode is larger than the optical wavelength. We follow the notation of [21] and employ the key vector $|A\rangle$ for representing a Jones vector polarized in the x - y plane. In this notation, the two fields at any point \mathbf{r} inside the fiber can be written as

$$\mathbf{E}_j(\mathbf{r}, t) = F_j(x, y) |A_j(z, t)\rangle \exp(i\beta_j z) \quad (5)$$

where $F_j(x, y)$ represents the fiber-mode profile and β_j is the propagation constant at the carrier frequency ω_j . The Jones vector $|A_j\rangle$ is a two-dimensional column vector representing the two components of the electric field in the x - y plane. The fiber-mode profiles can be taken to be nearly the same for the two fields, $F_j(x, y) \equiv F(x, y)$, which amounts to assuming the same effective core area a_{eff} for the two waves.

Using (1)–(5) in the Maxwell equations, integrating over the transverse coordinates in the x - y plane, and assuming $|A_j\rangle$ to be a slowly varying function of z so that we can neglect its second-order derivative with respect to z , we obtain the following vector form of the NLS equation:

$$\begin{aligned} \frac{\partial |A_j\rangle}{\partial z} + \beta_{1j} \frac{\partial |A_j\rangle}{\partial t} + \frac{i\beta_{2j}}{2} \frac{\partial^2 |A_j\rangle}{\partial t^2} \\ = \frac{i\gamma_j}{3} [2\langle A_j | A_j \rangle + |A_j^*\rangle \langle A_j^*| + 2\langle A_m | A_m \rangle \\ + 2|A_m\rangle \langle A_m| + 2|A_m^*\rangle \langle A_m^*|] |A_j\rangle \end{aligned} \quad (6)$$

where $j, m = 1$ or 2 ($j \neq m$), and the nonlinear parameter is defined as

$$\gamma_j \equiv \frac{n_2 \omega_j}{(ca_{\text{eff}})} = \frac{3\omega_j^2 \chi_{1111}^{(3)}}{(8c^2 \beta_j a_{\text{eff}})}. \quad (7)$$

Similar to the scalar case [1], the effects of fiber dispersion were included by expanding β_j in a Taylor series around the carrier frequency ω_j . The parameter $\beta_{1j} \equiv 1/v_{gj}$ is related to the group velocity while β_{2j} takes into account the effects of GVD inside the fiber. $\langle A |$ and $|A^*\rangle$ are Hermitian and complex conjugates of $|A\rangle$, respectively. In deriving (6), the fiber is assumed to be cylindrically symmetric without birefringence, and fiber losses are neglected. Real fibers have some residual birefringence that fluctuates along the fiber length and leads to polarization-mode dispersion (PMD). The PMD effects are well known in the absence of nonlinear effects [21] but they complicate the present analysis considerably and will be considered in a separate paper.

III. POLARIZATION EVOLUTION OF PUMP AND PROBE

Vector theory of XPM requires a solution of the two coupled vector NLS equations given in (6). This set of equations cannot be solved analytically, and one must use a numerical approach in general. To isolate the XPM-induced polarization effects as simply as possible, we make two simplifications in this section. First, we assume that the fiber length L is much shorter than the dispersion length $L_{Dj} = T_0^2/|\beta_{2j}|$ ($j = 1, 2$) so that we can neglect the effect of GVD temporarily. Second, we adopt a pump-probe configuration and assume that $|A_2\rangle$ is much weaker than $|A_1\rangle$. This is often the case in practice.

For simplicity, we also assume that the nonlinear parameters are nearly the same for the two waves, i.e., $\gamma_1 \approx \gamma_2 = \gamma$. We can then introduce a single nonlinear length $L_n = 1/(\gamma P_0)$ and normalize z as $\xi = z/L_n$, where P_0 is the peak power of the pump pulse. Introducing a reduced time variable in a frame moving with the probe pulse as $\tau = (t - \beta_{12}z)/T_0$, where T_0 is the width of the pump pulse, (6) can be simplified and take the form

$$\frac{\partial |A_1\rangle}{\partial \xi} + \mu \frac{\partial |A_1\rangle}{\partial \tau} = \frac{i}{3} (3p_0 - \mathbf{p}_3 \cdot \boldsymbol{\sigma}) |A_1\rangle \quad (8)$$

$$\frac{\partial |A_2\rangle}{\partial \xi} = \frac{2i}{3} [2p_0 + (\mathbf{p} - \mathbf{p}_3) \cdot \boldsymbol{\sigma}] |A_2\rangle \quad (9)$$

where $\mu = L_n/L_w$, $L_w = T_0/(\beta_{11} - \beta_{12})$ being the walkoff length, and $\mathbf{p}(\xi, \tau)$ represents the SOP of the pump pulse on the Poincaré sphere through the Stokes vector defined as

$$\mathbf{p}(\xi, \tau) = \frac{\langle A_1(\xi, \tau) | \boldsymbol{\sigma} | A_1(\xi, \tau) \rangle}{P_0}. \quad (10)$$

Also, $p_0(\xi, \tau) = \langle A_1(\xi, \tau) | A_1(\xi, \tau) \rangle / P_0$ represents the normalized temporal profile of the pump. The vector $\boldsymbol{\sigma}$ is defined using the unit vectors \hat{e}_j in the Stokes space as $\boldsymbol{\sigma} = \sigma_1 \hat{e}_1 + \sigma_2 \hat{e}_2 + \sigma_3 \hat{e}_3$, where σ_j ($j = 1, 2, 3$) are the three Pauli matrices [21]. Finally, $\mathbf{p}_3 = (\mathbf{p} \cdot \hat{e}_3) \hat{e}_3$ is the third component of the vector \mathbf{p} (corresponding to circular polarization). Light is linearly polarized whenever $p_3 = 0$ because \mathbf{p} then lies entirely in the equatorial plane of the Poincaré sphere.

The pump equation is much easier to solve in the Stokes space. We first use the definition of \mathbf{p} to obtain an equation for it. Using the identity [21]

$$\sigma(\mathbf{a} \cdot \boldsymbol{\sigma}) = \mathbf{a} \overleftrightarrow{\mathbf{I}} + i\mathbf{a} \times \boldsymbol{\sigma}$$

the pump SOP governed by \mathbf{p} is found to evolve as

$$\frac{\partial \mathbf{p}}{\partial \xi} + \mu \frac{\partial \mathbf{p}}{\partial \tau} = \frac{2}{3} \mathbf{p}_3 \times \mathbf{p}. \quad (11)$$

This equation is easy to solve and provides the following solution for the Stokes vector of the pump:

$$\mathbf{p}(\xi, \tau) = \exp\left[\left(\frac{2\xi}{3}\right) \mathbf{p}_3 \times\right] \mathbf{p}(0, \tau - \mu\xi) \quad (12)$$

where the notation $\exp(\mathbf{p}_3 \times)$ is from [21] and should be interpreted in terms of a series expansion. Physically, it represents a rotation of the Stokes vector around \mathbf{p}_3 . This rotation is known as NPR, as mentioned earlier.

In the absence of GVD, the pump pulse remains unchanged along the fiber but it separates from the probe because of pulse walkoff. Its SOP also changes because of SPM as indicated in (12). If the pump is linearly or circularly polarized initially, its SOP does not change along the fiber. For an elliptically polarized pump, SPM-induced NPR changes its SOP continuously. As SPM is power dependent, NPR depends on the temporal profile, and different part of the pump pulse acquire different SOPs. As will be seen later, such *intrapulse* polarization effects have a profound effect on the probe evolution.

We now consider the XPM-induced polarization effects on the probe. For this purpose, we introduce the Stokes vector of the probe as

$$\mathbf{s}(\xi, \tau) = \frac{\langle A_2(\xi, \tau) | \boldsymbol{\sigma} | A_2(\xi, \tau) \rangle}{S_0} \quad (13)$$

where S_0 represents the peak power of the probe. We then follow the procedure used earlier for the pump to obtain the following equation for \mathbf{s} :

$$\frac{\partial \mathbf{s}}{\partial \xi} = -\frac{4}{3} (\mathbf{p} - \mathbf{p}_3) \times \mathbf{s}. \quad (14)$$

This equation shows that the pump rotates the probe's Stokes vector around $\mathbf{p} - \mathbf{p}_3$, a vector that lies in the equatorial plane of the Poincaré sphere. As a result, if the pump is circularly polarized initially, XPM effect becomes polarization independent since $\mathbf{p} - \mathbf{p}_3 = 0$. On the other hand, if the pump is linearly polarized, $\mathbf{p}_3 = 0$, and \mathbf{p} remains fixed in the Stokes space. However, even though the pump SOP does not change in this case, probe SOP can change through XPM-induced NPR. If the pump wave is in the form of a pulse, XPM will induce different amount of NPR on the different parts of the probe pulse, resulting in nonuniform polarization along the probe pulse profile. The XPM-induced NPR effects become quite complicated when the pump is elliptically polarized since pump SOP itself changes through SPM. Such polarization changes impact the XPM-induced chirp, and the spectral profile of the probe exhibits much more complicated structure compared with the scalar case. We focus on the spectral effects in the next section.

IV. POLARIZATION-DEPENDENT SPECTRAL BROADENING

In general, (9) needs to be solved numerically except when the pump maintains its SOP. As discussed earlier, this happens when the pump pulse is linearly or circularly polarized initially. In the following discussion, we focus on two specific cases. In one case, both pump and probe are linearly polarized at the input end but the probe is oriented at an angle θ with respect to the pump. In the second case, the pump SOP is elliptical initially but the probe is linearly polarized. We use the major and minor axis (aligned with the x and y axes, respectively) of this ellipse as the basis in which the SOP of the pump and probe is represented in the Jones space. Assuming a Gaussian shape for both pulses, the Jones vectors for the two input fields have the form

$$\begin{aligned} |A_1(0, \tau)\rangle &= \begin{bmatrix} \cos \phi \\ i \sin \phi \end{bmatrix} \sqrt{P_0} \exp\left(-\frac{\tau^2}{2}\right) \\ |A_2(0, \tau)\rangle &= \begin{bmatrix} \cos \theta \\ \sin \theta \end{bmatrix} \sqrt{S_0} \exp\left(-\frac{\tau^2}{2r^2}\right) \end{aligned} \quad (15)$$

where ϕ is the ellipticity angle for the pump and $r = T_2/T_0$ is the relative width of the probe compared to the pump. Using this form as an input, we first solve (9) numerically to obtain $|A_2(\xi, \tau)\rangle$ and then calculate the spectrum for the orthogonally polarized components of the probe by taking the Fourier transform.

Consider first the case of a linearly polarized pump along the x axis by setting $\phi = 0$. As SPM does not affect the pump SOP in this case, the analytical solution of the probe field is found to be

$$|A_2(\xi, \tau)\rangle = \sqrt{S_0} \begin{bmatrix} \cos \theta \exp\left(\frac{i\Phi_n}{3}\right) \\ \sin \theta \exp\left(\frac{i\Phi_n}{3}\right) \end{bmatrix} \exp\left(-\frac{\tau^2}{2r^2}\right) \quad (16)$$

where $\Phi_n(\xi, \tau) = 2 \int_0^\xi p_0(\xi', \tau) d\xi'$ is the XPM-induced nonlinear phase shift. The probe pulse shape does not change in the absence of GVD, as expected. However, its SOP changes and it acquires a nonlinear time-dependent phase shift that chirps the probe pulse and leads to spectral broadening. Notice that the XPM-induced phase shift for the y -polarized component is one third of that the copolarized one because of the reduction in the XPM coupling efficiency. This is a well-known feature of XPM [1].

Fig. 1(a) shows the probe spectra along the x (solid curve) and y (dashed curve) axes for a fiber of length $L = 5\pi L_n$ ($\xi = 5\pi$) assuming that the probe is polarized at $\theta = 45^\circ$ and that the two input pulses have the same width ($r = 1$). The walkoff length is chosen to be one half of the total fiber length ($L_w = L/2$). The copolarized component has a much broader spectrum with an oscillatory structure than the orthogonally polarized one. When the spectrum is measured without placing a polarizer in front of the photodetector, one would record the total spectral intensity shown by a thin solid line in Fig. 1. However, it is important to realize that the SOP is not the same for all spectral peaks. As seen in Fig. 1, The leftmost peak is x polarized whereas the dominant peak in the center is mostly y polarized in this case. This spectral nonuniformity of the SOP is a direct consequence of the XPM-induced NPR.

When the SOP of the input pump is changed to elliptical, the XPM effect changes considerably because even the pump SOP

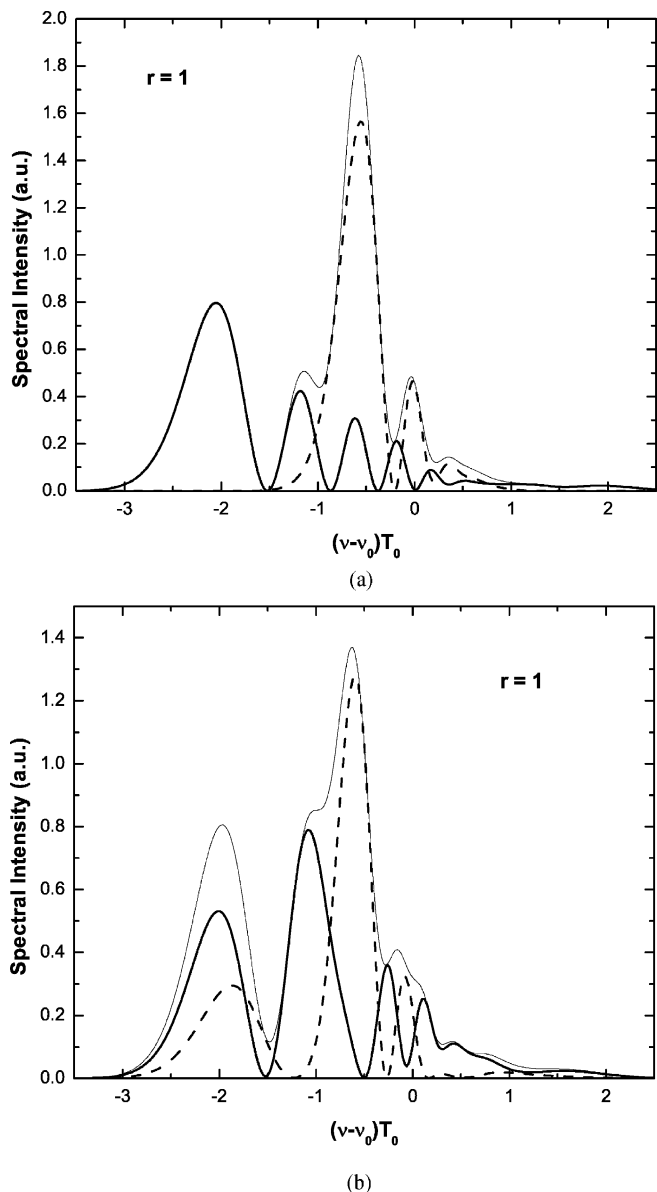


Fig. 1. Spectral broadening of a probe pulse linearly polarized at $\theta = 45^\circ$ when pump pulse is (a) linearly polarized along the x axis or is (b) elliptically polarized. The solid and dashed curves show the spectra for x - and y - polarized components of the probe, respectively. The thin solid curve shows the whole probe spectrum.

is not maintained along the fiber. The probe pulse spectra in this case are shown in Fig. 1(b) for an input ellipticity angle of $\phi = 20^\circ$. All other parameters are kept the same. A comparison of Fig. 1(a) and (b) gives an idea how much probe spectrum can change with a small change in the pump SOP. A new feature is that even the temporal probe profiles are now different for the x and y polarized components even though the total power profile remains the same as long as GVD effects are negligible. This feature is shown in Fig. 2. The pulse shapes for the two polarized components exhibit a multipeak structure such that the total power at any time adds up to the input value. The physical origin of this behavior is the SPM-induced NPR for the pump pulse. As the pump SOP evolves, the probe SOP changes in a complex manner. Fig. 2 shows the temporal evolution of the SOP for the pump (gray curve) and probe (black curve). The left and right

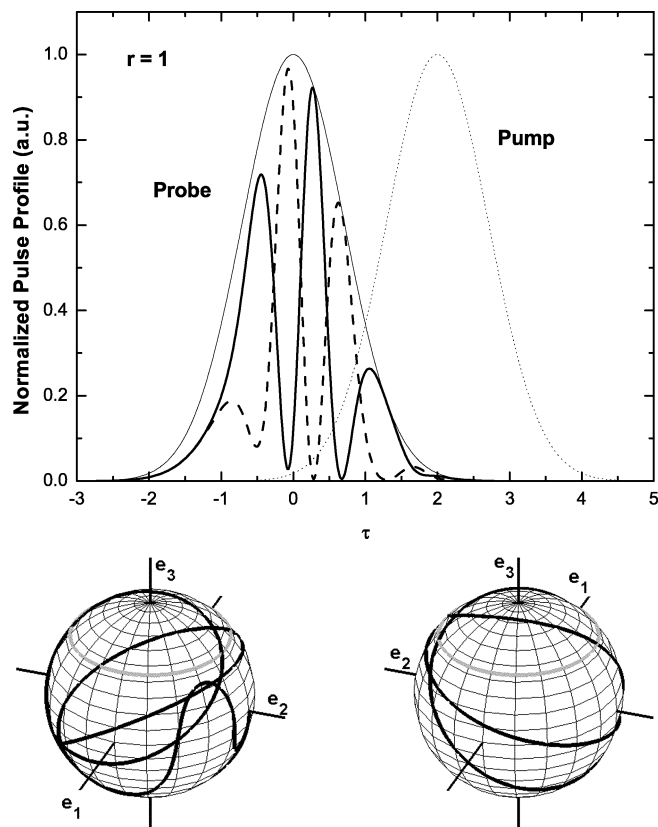


Fig. 2. Temporal profiles of x -polarized (solid curve) and y -polarized (dashed curve) components of the probe under conditions of Fig. 1(b). The thin solid curve shows the total probe power. The dotted curve shows pump pulse assumed to be elliptically polarized. Temporal evolution of the SOP of the pump (gray curve) and probe (black curve). The left and right parts show the front and back faces of the sphere, respectively.

parts show the front and back faces of the Poincaré sphere, respectively. The pump Stokes vector traces a circle in time as it rotates around the \hat{e}_3 axis. However, the time-dependent probe Stokes vector follows the black trajectory and exhibits a quite complicated pattern. The temporal structure seen in Fig. 2 stems from this complex polarization behavior.

The spectral asymmetry seen in Fig. 1 is a direct consequence of pulse walk off [1]. When the pump and probe pulses separate rapidly because of a short walkoff length, the main affect of XPM is to induce a spectral shift without changing the pulse spectrum drastically. The NPR effects studied here lead to different XPM-induced spectral shifts for the two polarization components of the probe. This feature is seen clearly in Fig. 3 obtained using the same parameters as in Fig. 1 except that the probe pulse is half as wide as pump ($r = 1/2$) and, thus, separates rapidly from the pump pulse. The pump is assumed to be linearly polarized at the input end. The whole spectrum of the probe pulse (thin solid line) exhibits a two-peak structure. However, the two spectral peaks are orthogonally polarized. Indeed, the individual spectra for the two polarization components are not broadened much (solid and dashed curves) except that their central frequencies are shifted by different amounts because of the XPM effects. As expected, the copolarized component undergoes a much larger shift compared with the orthogonally polarized one. This effect may be useful for polarization-induced

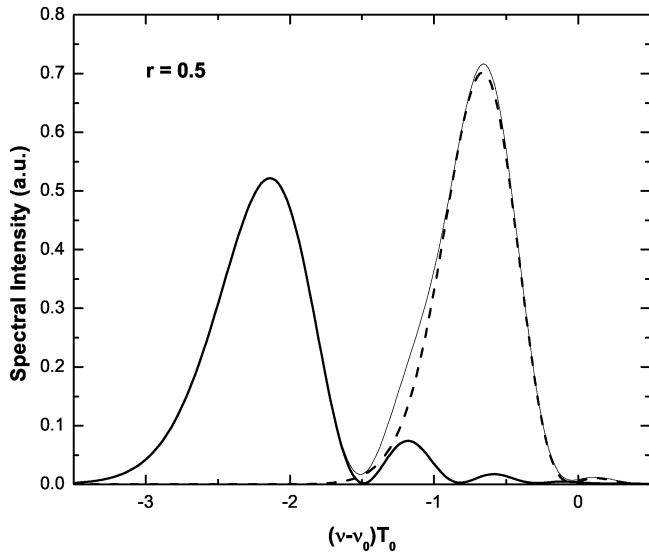


Fig. 3. Probe spectra under conditions of Fig. 1(a) except that the probe is only half as wide as the pump pulse ($r = 0.5$).

switching. By placing a filter at the shifted position, the probe pulse can be turned on or off by simply changing the pump (or signal) polarization.

V. POLARIZATION-DEPENDENT PULSE SPLITTING AND PULSE COMPRESSION

The preceding analysis assumed that the fiber was much shorter than the dispersion length such that both the pump and probe pulses maintained their temporal profile. In this section we relax this assumption and focus on the XPM-induced polarization-dependent temporal effects. In the presence of GVD, an extra term appears in (8) and (9)

$$\frac{\partial|A_1\rangle}{\partial\xi} + \mu \frac{\partial|A_1\rangle}{\partial\tau} + \frac{i\eta_1}{2} \frac{\partial^2|A_1\rangle}{\partial\tau^2} = \frac{i}{3}(3p_0 - \mathbf{p}_3 \cdot \boldsymbol{\sigma})|A_1\rangle \quad (17)$$

$$\frac{\partial|A_2\rangle}{\partial\xi} + \frac{i\eta_2}{2} \frac{\partial^2|A_2\rangle}{\partial\tau^2} = \frac{2i}{3}[2p_0 + (\mathbf{p} - \mathbf{p}_3) \cdot \boldsymbol{\sigma}]|A_2\rangle \quad (18)$$

where $\eta_j = L_n/L_{dj}$ is inversely related to the dispersion length $L_{dj} = T_0^2/|\beta_{2j}|$ ($j = 1, 2$). In the following discussion, we assume for simplicity that $\beta_{21} = \beta_{22} \equiv \beta_2$ so that $L_{d1} = L_{d2} \equiv L_d$. This is the case for a dispersion-flattened fiber or when the pump and probe wavelengths do not differ by more than a few nanometers.

Three length scales—nonlinear length L_n , walkoff length L_w , and dispersion length L_d —characterize the interplay between GVD and XPM. It is well known that XPM-induced chirp can cause the probe pulse to break up or to compress depending on the relative magnitudes of the three lengths [1]. If $L_n \ll L_w \ll L_d$ and the fiber exhibits normal dispersion, small dispersion will cause probe pulse to break asymmetrically. If $L_w \geq L_d$ and the fiber dispersion is anomalous, probe pulse can be compressed through XPM-induced chirp. As we shall see in this section, situation becomes more complicated in the vector case since

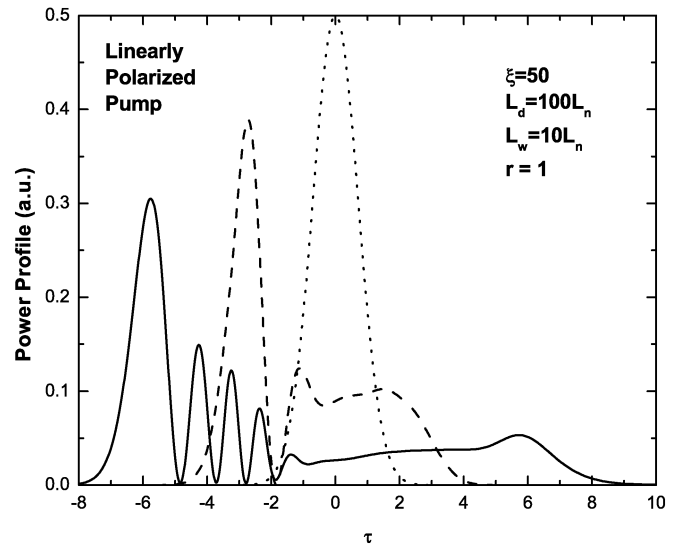


Fig. 4. Temporal profiles of x -polarized (solid curve) and y -polarized (dashed curve) components of the probe under conditions of Fig. 1(a) at a distance of $50L_n$ in the normal GVD regime. The pump and probe pulses have a Gaussian shape and the same initial width. The solid and dashed curves show the copolarized and orthogonally polarized component, respectively. The dotted curves shows the initially identical probe pulse profile for both polarization components ($\theta = 45^\circ$).

the two polarization components of the probe propagate in qualitatively different ways under the combined effect of fiber dispersion and XPM. We study the polarization effects by solving the two vector NLS equations numerically using the split-step Fourier method [1]. Note that this amounts to solving four coupled NLS equations.

We first consider the normal-dispersion case ($\beta_2 > 0$). Fig. 4 shows an example of pulse breakup inside a fiber of length $L = 50L_n$ for the linear and elliptically polarized pumps using $L_d = 100L_n$ and $L_w = 10L_n$. Normal dispersion of the fiber causes the probe pulse to break up asymmetrically. An oscillatory structures develops near the leading or trailing edge of the probe pulse depending on how the pump walks away from the probe pulse. However, the details of wave breaking are quite different for the two polarization components of the probe. In the case of a linearly polarized pump, the copolarized component (solid curve) of the probe exhibits much more oscillatory structure than the orthogonally polarized one (dashed curve) because the XPM-induced chirp and spectral broadening is larger for it. This feature can be verified experimentally by placing a polarizer before the photodetector and noticing that the oscillatory structure changes as polarizer is rotated. When the pump pulse is elliptically polarized, the polarization dependence of probe profile is reduced but remains measurable.

Next we focus on the XPM-induced pulse compression in a fiber with anomalous dispersion ($\beta_2 < 0$). Fig. 5 shows the results obtained under the conditions identical of Fig. 4 except that dispersion length is only five times as long as the nonlinear length ($L_d = 5L_n$). When the pump is linearly polarized, the combined effects of XPM and GVD compress the copolarized component of the probe by a large amount (solid curve). However, at the same time, the orthogonally polarized component undergoes severe broadening (dashed curve). This strange behavior is related to the reduced XPM interaction occurring

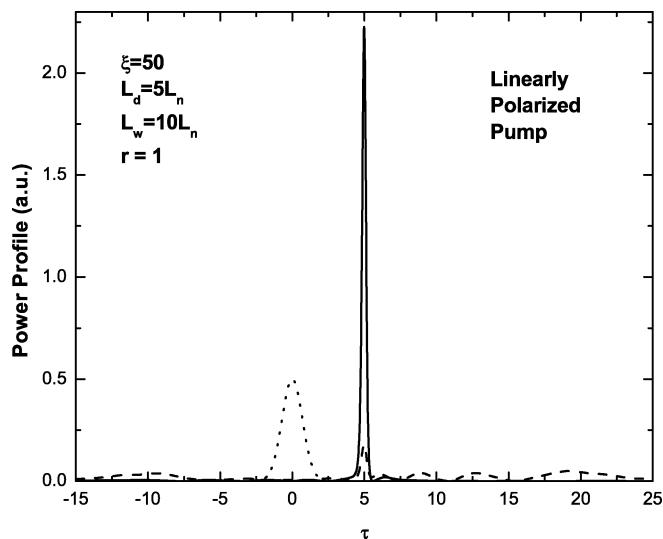


Fig. 5. Same as in Fig. 4 except that $L_d = 5L_n$ and both pulses propagate in the anomalous-GVD regime of the fiber. The solid and dashed curves show the copolarized and orthogonally polarized component, respectively. The dotted curves shows the initially identical probe pulse profile for both polarization components ($\theta = 45^\circ$).

when the pump and probe are orthogonally polarized. The total probe profile exhibits a narrow central copolarized peak with a wide wing that is orthogonally polarized. The wing can be suppressed by using a polarizer aligned with the pump SOP. When the pump is elliptically polarized, such polarization effects persist but become less dramatic because of SPM-induced changes in the pump SOP.

Finally, we consider XPM-induced splitting of a probe pulse. As discussed in Section III, polarization-dependent XPM not only change the spectrum of the probe, but also shift its central frequency. This is seen clearly in Fig. 5 where the probe has moved away from its initial position because of the spectral shift. In general, this spectral shift is different for the two polarization components of the probe. This spectral difference is transferred to the pulse position through differential group delay since the two polarization components propagate with different group velocities. Fig. 6 shows an example of pulse splitting under the same conditions used for Fig. 5 except that the fiber exhibits weak anomalous dispersion and the dispersion length for the pump pulse is 400 times longer than the nonlinear length ($L_d = 400L_n$). As the width of the probe pulse is half of the pump, its own dispersion length is 100 times longer than the nonlinear length. When the pump is linearly polarized, the spectral shift of the copolarized component (solid curve) occurs toward the low-frequency side and is much larger than that of the orthogonally polarized one (dashed curve). As a result, the copolarized component of the probe pulse propagates slower than the orthogonally polarized one, and the two are separated in the time domain, as seen in Fig. 6. The probe pulse will appear to have two distinct peaks when its total intensity is measured as a function of time. However, the two peaks have orthogonal polarizations, and can be separated by using a polarizing beam splitter. Similar features are observed for an elliptically polarized pump, although the separation between the two peaks depends on the ellipticity angle.

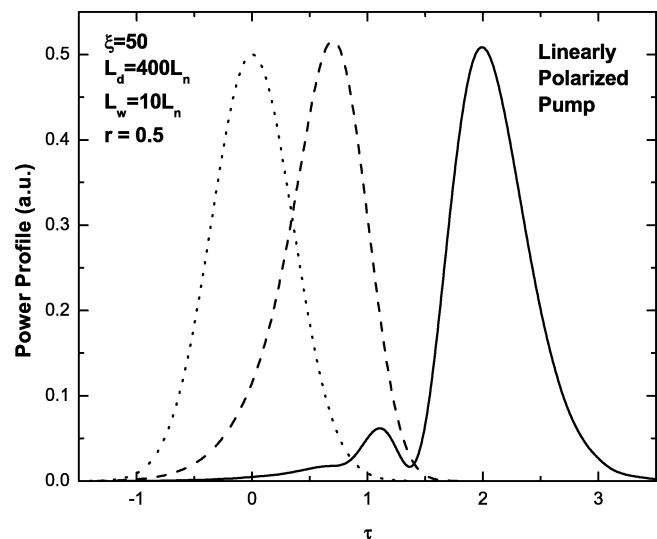


Fig. 6. Same as in Fig. 4 except that both pulses propagate in the anomalous-GVD regime of the fiber and probe pulse is only half as wide as the pump pulse ($r = 0.5$). The solid and dashed curves show the copolarized and orthogonally polarized component, respectively. The dotted curves shows the initially identical probe pulse profile for both polarization components ($\theta = 45^\circ$).

VI. CONCLUSION

In this paper we have developed a vector theory of XPM capable of describing nonlinear coupling between two pulses of different wavelengths and arbitrary states of polarization. We have focused for simplicity on the pump-probe configuration in which probe pulse is much weaker than the pump pulse and used it to investigate the temporal and spectral polarization effects occurring inside an optical fiber. Using the Stokes-vector formalism we show that pump polarization does not change when pump pulse is linearly or circularly polarized. However, the probe polarization changes in general through XPM-induced NPR. In the absence of dispersion-induced probe broadening, such nonlinear changes in the probe polarization do not affect the temporal shape of the probe pulse but produce a multipeak spectrum whose different spectral peaks have different states of polarization. When dispersive effects are included, even the shape of the probe pulse becomes polarization dependent, i.e., different parts of the pulse have different states of polarization. Such nonlinear polarization effects lead to novel phenomena such as polarization-dependent compression and splitting of the probe pulse.

REFERENCES

- [1] G. P. Agrawal, *Nonlinear Fiber Optics*, 3rd ed. San Diego, CA: Academic, 2001.
- [2] J. I. Gersten, R. R. Alfano, and M. Belic, "Combined stimulated Raman scattering and continuum self-phase modulation," *Phys. Rev. A, Gen. Phys.*, vol. 21, pp. 1222–1224, Apr. 1980.
- [3] M. N. Islam, L. F. Mollenauer, R. H. Stolen, J. R. Simpson, and H. T. Shang, "Cross-phase modulation in optical fibers," *Opt. Lett.*, vol. 12, pp. 625–627, Aug. 1987.
- [4] G. P. Agrawal, "Modulation instability unduced by cross-phase modulation," *Phys. Rev. Lett.*, vol. 59, pp. 880–883, Aug. 1987.
- [5] R. R. Alfano, P. L. Baldeck, F. Raccach, and P. P. Ho, "Cross-phase modulation measured in optical fibers," *Appl. Opt.*, vol. 26, pp. 3491–3492, Sept. 1987.

- [6] D. Schadt and B. Jaskorzynska, "Suppression of Raman self-frequency shift by cross-phase modulation," *J. Opt. Soc. Amer. B, Opt. Phys.*, vol. 5, pp. 2374–2378, Nov. 1988.
- [7] R. R. Alfano and P. P. Ho, "Self-, cross-, and induced-phase modulations of ultrashort laser pulse propagation," *IEEE J. Quantum Electron.*, vol. 24, pp. 351–364, Feb. 1988.
- [8] P. L. Baldeck, P. P. Ho, and R. R. Alfano, *The Supercontinuum Laser Source*, R. R. Alfano, Ed. New York: Springer-Verlag, 1989, ch. 4.
- [9] T.-K. Chiang, N. Kagi, M. E. Marhic, and L. G. Kazovsky, "Cross-phase modulation in fiber links with multiple optical amplifiers and dispersion compensators," *J. Lightwave Technol.*, vol. 14, pp. 249–260, Mar. 1996.
- [10] A. V. T. Cartaxo, "Cross-phase modulation in intensity modulation-direct detection WDM systems with multiple optical amplifiers and dispersion compensators," *J. Lightwave Technol.*, vol. 17, pp. 178–190, Feb. 1999.
- [11] R. Hui, K. R. Demarest, and C. T. Allen, "Cross-phase modulation in multispan WDM optical fiber systems," *J. Lightwave Technol.*, vol. 17, pp. 1018–1026, June 1999.
- [12] P. Bayvel and R. Killely, *Optical Fiber Telecommunications IV B*, I. P. Kaminov and T. Li, Eds. San Diego, CA: Academic, 2002, ch. 13.
- [13] G.-H. Duan, *Semiconductor Lasers: Past, Present, and Future*, G. P. Agrawal, Ed. New York: AIP, 1995, ch. 10.
- [14] P. Ohlen, B. E. Olsson, and D. J. Blumenthal, "Wavelength dependence and power requirements of a wavelength converter based on XPM in a dispersion-shifted optical fiber," *IEEE Photon. Technol. Lett.*, vol. 12, pp. 522–524, May 2000.
- [15] V. E. Perlin and H. G. Winful, "Nonlinear pulse switching using cross-phase modulation and fiber Bragg gratings," *IEEE Photon. Technol. Lett.*, vol. 13, pp. 960–962, Sept. 2001.
- [16] B. E. Olsson and D. J. Blumenthal, "All-optical demultiplexing using fiber cross-phase modulation and optical filtering," *IEEE Photon. Technol. Lett.*, vol. 13, pp. 875–877, Aug. 2001.
- [17] B. C. Sarker, T. Yoshino, and S. P. Majumder, "All-optical wavelength conversion based on cross-phase modulation in a single-mode fiber and a Mach-Zehnder interferometer," *IEEE Photon. Technol. Lett.*, vol. 14, pp. 340–342, Mar. 2002.
- [18] C. Schubert, J. Berger, S. Diez, H. J. Ehrke, R. Ludwig, U. Feiste, C. Schmidt, H. G. Weber, G. Toptchivski, S. Randel, and K. Petermann, "Comparison of interferometric all-optical switches for demultiplexing applications in high-speed OTDM systems," *J. Lightwave Technol.*, vol. 20, pp. 618–624, Apr. 2002.
- [19] G. P. Agrawal, *Applications of Nonlinear Fiber Optics*. San Diego, CA: Academic, 2001.
- [20] R. W. Boyd, *Nonlinear Optics*, 2nd ed. San Diego, CA: Academic, 2003.
- [21] J. P. Gordon and H. Kogelnik, "PMD fundamentals: Polarization mode dispersion in optical fibers," in *Proc. Nat. Acad. Sci.*, vol. 97, 2000, pp. 4541–4550.



Qiang Lin received the B.S. degree in applied physics and the M.S. degree in optics from Tsinghua University, Beijing, China, in 1996 and 1999, respectively. He is currently pursuing the Ph.D. degree at the Institute of Optics, University of Rochester, Rochester, NY.

His research interests include nonlinear fiber optics, polarization mode dispersion, optical communications, and ultrafast optics.



Govind P. Agrawal (M'83–SM'86–F'96) received the B.S. degree from the University of Lucknow, India, in 1969, and the M.S. and Ph.D. degrees from the Indian Institute of Technology, New Delhi, in 1971 and 1974, respectively.

After holding positions at the Ecole Polytechnique, Palaiseau, France, the City University of New York, New York, and the AT&T Bell Laboratories, Murray Hill, NJ, Dr. Agrawal joined the faculty of the Institute of Optics at the University of Rochester, Rochester, NY in 1989, where he is currently a

Professor of Optics. His research interests focus on optical communications, nonlinear optics, and laser physics. He is an author or coauthor of more than 300 research papers, several book chapters and review articles, and five books entitled *Semiconductor Lasers* (Norwell, MA: Kluwer Academic, 2nd ed., 1993), *Fiber-Optic Communication Systems* (New York: Wiley, 3rd ed., 2002), *Nonlinear Fiber Optics* (New York: Academic, 3rd ed., 2001), *Applications of Nonlinear Fiber Optics* (New York: Academic, 2001), and *Optical Solitons: From Fibers to Photonic Crystals* (New York: Academic, 2003). He has also edited two books: *Contemporary Nonlinear Optics* (New York: Academic, 1992) and *Semiconductor Lasers: Past, Present and Future* (New York: AIP, 1995).

Dr. Agrawal is a Fellow of the Optical Society of America (OSA). He has participated multiple times in organizing technical conferences sponsored by OSA and IEEE. He was the Program Co-Chair in 1999 and the General Co-Chair in 2001 for the Quantum Electronics and Laser Science Conference. He was a Member of the Program Committee in 2004 for the Conference on Lasers and Electrooptics (CLEO).